

ECE 445
Fall 2025
Final Report

Heart Restart

Team:

William Mendez (@illinois.edu)

Ethan Moraleda (@illinois.edu)

Brian Chiang (@illinois.edu)

TA: Frey Zhao

Professor: Arne Fliflet

December 10, 2025

Table of Contents

1 Introduction.....	2
2 Design.....	4
2.1 Design Procedure.....	4
2.1.1 ECG.....	4
2.1.2 Impedance.....	4
2.1.3 Power Unit.....	5
2.1.4 Control Unit.....	6
2.2 Design Details.....	7
2.2.1 ECG.....	7
2.2.2 Impedance.....	8
2.2.3 Power Unit.....	10
2.2.4 Control Unit.....	11
Over-voltage Protection.....	11
Button Debounce.....	11
Software.....	12
3 Verification.....	14
3.1 ECG.....	14
3.2 Impedance.....	14
3.3 Power Unit.....	15
3.4 Control Unit.....	16
Debounce.....	16
LCD and Button Functionality.....	16
Apply Digital Signal Processing to the ECG input.....	17
4 Costs and Schedule.....	18
5 Conclusion.....	19
6 References.....	20
7 Appendix.....	23
Electrocardiogram.....	23
Bio Impedance Tracking.....	24
Control System.....	25
Power Regulation Unit.....	27

1 Introduction

Research has shown that defibrillators delivering a single shock achieve relatively low survival rates of only 13.3%. In contrast, Double Sequential External Defibrillators (DSED)—which deliver two rapid consecutive shocks—significantly improve survival rates to 30.4%. However, DSED currently requires two separate defibrillators, making it impractical in real-world emergencies, particularly in ambulances where only one defibrillator is typically available. Furthermore, the precise millisecond-level timing required between each shock further complicates the coordination of the two devices. Additionally, most commercially available defibrillators lack impedance measurement capabilities, which prevents them from automatically adjusting shock strength based on patient-specific characteristics, such as body type and chest impedance. Those that do include such sensing capabilities tend to be larger, more complex, and significantly more expensive, which limits their accessibility in emergency medical settings.

Due to the time and safety constraints associated with developing a complete AED, our project focuses on implementing the core sensing subsystem required for a future Double Sequential External Defibrillator. Specifically, we created an ECG module for heart-rate detection and an impedance-sensing module capable of measuring patient chest impedance. For demonstration, the system includes an LCD interface that allows the user to toggle between real-time BPM and impedance readings. A custom power board and microcontroller platform were designed to supply regulated power, acquire and process sensor data, and manage the user display. Figure 1 shows the high-level system block diagram, which includes the Power Module, Control Module, ECG Module, and Impedance Module.

Heart Restart PCB Block Diagram

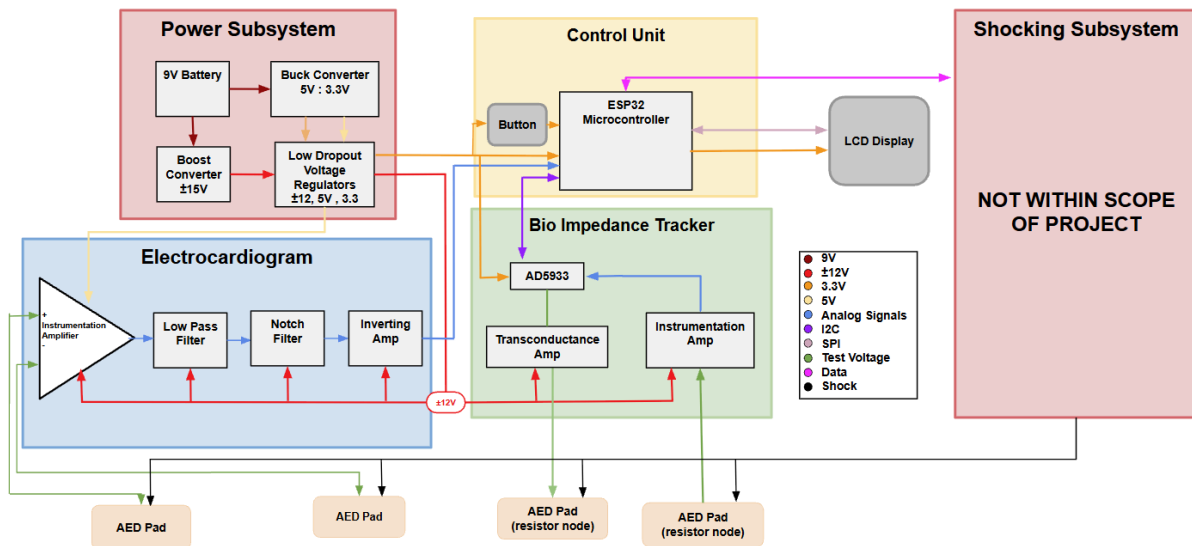


Figure 1: Block Diagram

As shown in the block diagram in Figure 1, each subsystem corresponds directly to the high-level performance requirements outlined in the final project proposal. The ECG module was required to detect heart rate and condition, amplify the resulting signal for microcontroller processing, and achieve a measurement accuracy of approximately 2.5%. The impedance-sensing module was specified to measure chest impedance with a target accuracy of 5%. In addition, the system was required to display both BPM and impedance values on an integrated display to support clear, immediate interpretation during operation. These requirements served as the basis for defining the Power, Control, ECG, and Impedance Modules within the overall system architecture.

When comparing the most recent block diagram to the original design concept, the functional relationships among modules remained consistent throughout development. However, several block-level modifications were introduced during the semester due to practical implementation constraints, component behavior, and insights gained during subsystem testing. The main changes were in the power block, where we included both boost and buck converters, and in the ECG, where we added an inverting amplifier at the final stage. We also added the Shocking Subsystem as a block to show the purpose of our project.

2 Design

2.1 Design Procedure

2.1.1 ECG

The ECG is designed to read the heart's voltage signal, amplify and filter it, and send the analog signal to the microcontroller for processing and heart rate measurement. Our design is based on a design from the internet, specifically the modules within the ECG itself. Our ECG is divided into four main parts: instrumentation amplifier, notch filter, low-pass filter, and inverting amplifier.

There are many ECG designs possible; however, we chose this configuration because it had fewer parts than the others. The other designs had more filters and amplifiers; however, our four modules already cover the bulk of filtering and amplification, compared to the more elaborate, larger designs. Another reason for the simpler design was that the ECG output signal was already fed into the microcontroller's DSP, so there was little need for additional filtering.

The design and component selection for the ECG are crucial, as the voltages from the heart fall roughly in the mV to μ V range, with many parasitic signals interfering with the signal. Thus, we chose an instrumentation amplifier with a gain of 1000, a notch filter to remove 60 Hz interference, and a low-pass filter to provide additional filtering. To design the filters, we utilized the TI filter design tool and filter tutorials to determine topologies, equations, and simulation results.

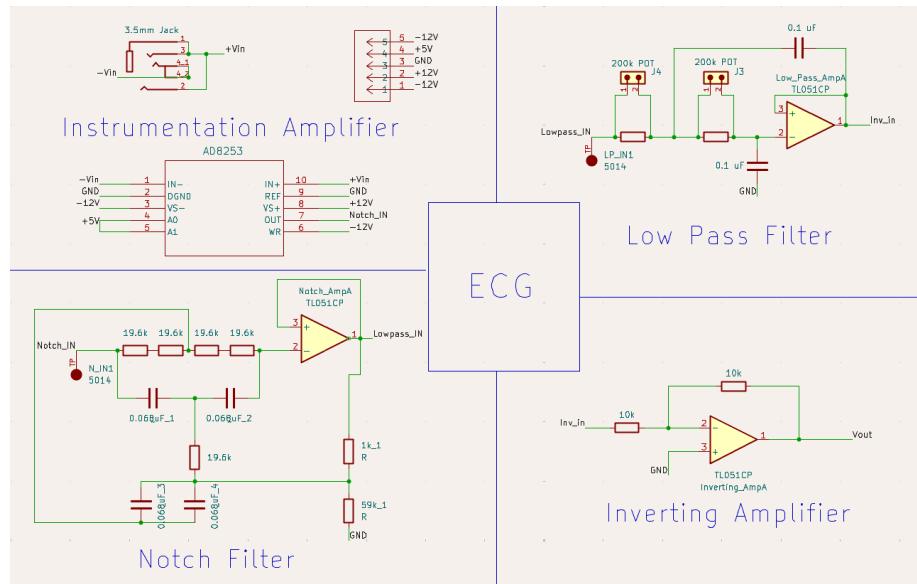


Figure 2: ECG Schematic

2.1.2 Impedance

The impedance module was based on the AD5933 IC. This IC generates a programmable sinusoidal signal that is then sent to simulate the unknown impedance. This resulting current is then converted back to a voltage by the internal transimpedance amplifier with an external feedback resistor to set the measurement gain. The voltage is digitized by a 12-bit ADC and

processed by an on-chip DSP, which performs a discrete Fourier transform to extract the real and imaginary components of the resistance.

We chose the AD5933 because there were numerous designs online that used the IC; however, most measured much higher impedances than we were aiming for. We could design a circuit that allows us to measure smaller impedances within safe current limits across the human body, at less than a couple of hundred μA .

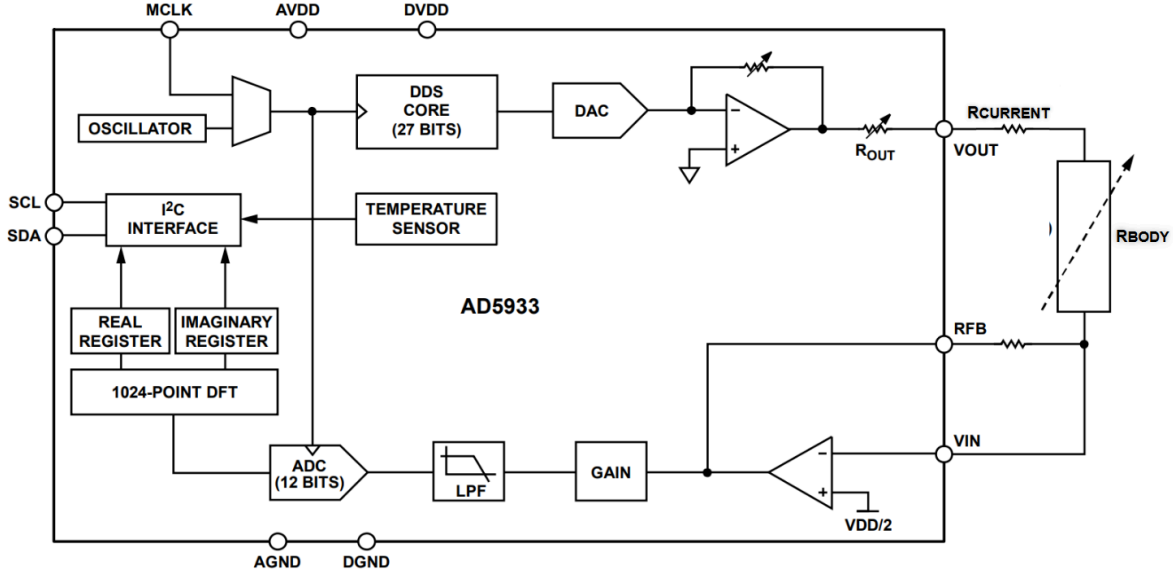


Figure 3: AD5933 Schematic

2.1.3 Power Unit

The power unit was designed to supply optimal voltages for each powered element within all other modules. Using a 9V battery, we can use the same power source as current AEDs and quickly replace it when depleted.

Our power unit has four outputs. +12V, -12V, 5V, and 3.3V. At each voltage level, a DC buck or boost converter and a load regulator. To ensure stability, we also used capacitors to filter out some of the switching noise from the isolated DC-DC converters. The ripple voltage with these caps can be calculated using the following equation:

$$\Delta V = \frac{I\Delta t}{C} = \frac{I\Delta t}{0.1\mu F + 10\mu F} \quad \text{Eq: 1}$$

The capacitor sizes we chose were 0.1 μF and 10 μF ceramic capacitors. 0.1 μF ceramic capacitors act as high-frequency decouplers because they have very low effective series resistance and inductance and are very effective at filtering high-frequency noise. This helps suppress the switching spikes from the converter's internal transformer and rectifiers. The 10 μF ceramic capacitors help eliminate low-frequency ripple and, due to their higher capacitance, provide most of the energy storage during load transients. Having only the larger capacitor would

introduce too much ESL to the circuit. An example of these caps placements can be seen in the following figure.

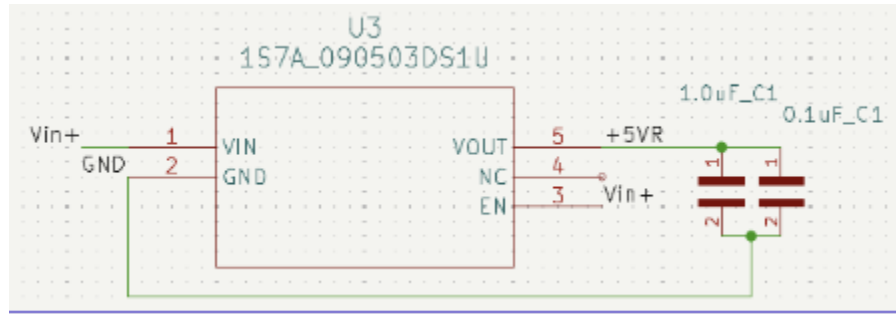


Figure 4: 9-5V LDO

We evaluated several topologies using different linear regulators and non-isolated converters, but chose isolated DC-DC converters for their efficiency, noise isolation, and voltage flexibility.

2.1.4 Control Unit

The control unit is based on the ESP32-S3-DevKitC-1 development board. The ESP32-S3 platform was chosen for its simplicity, high clock speed, ample GPIO availability, and overall suitability for embedded control applications. Additionally, this board was readily available for us to borrow for the semester. Several components from the DevKitC reference schematic were removed to simplify the design for our specific application. In their place, a few custom circuits were added to support the system's required features. Most notably, an overvoltage protection stage was included on the ECG analog output to ensure safe operation if the input exceeds the ESP32-S3's 3.3 V limit. Additionally, a debounced push-button was incorporated to allow the user to toggle between ECG and impedance measurement modes. These additions, along with the complete control unit schematic and the finished PCB, are shown in Figure 5.

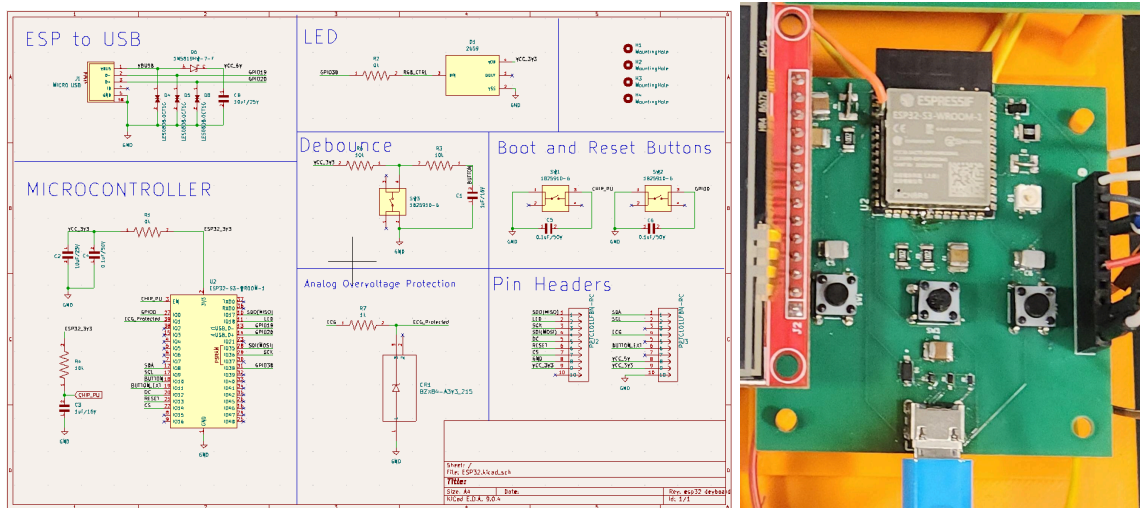


Figure 5: Control Unit Schematic and PCB

2.2 Design Details

2.2.1 ECG

The first module of the ECG is an instrumentation amplifier. This instrumentation amplifier, the AD8253, has a programmable gain, which we set to 1000 permanently. The reason is to amplify the roughly 1 mV peak-to-peak signal from the body; 1 mV is close to the maximum voltage we will see from the body, according to our medical student mentors.

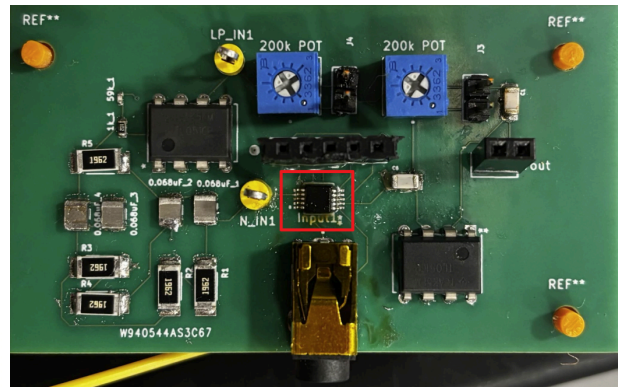
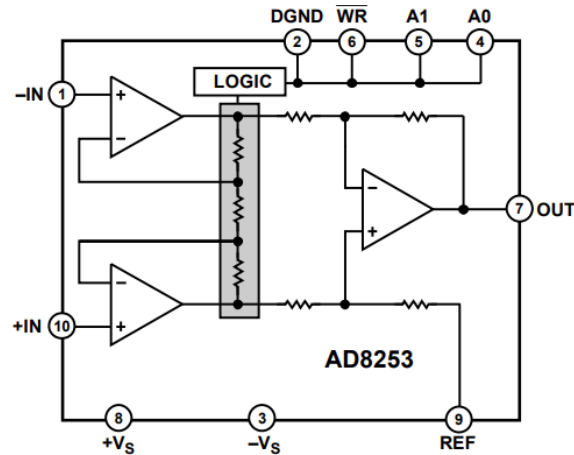


Figure 6: AD8253 Schematic and Location on PCB

The second module of the ECG is the notch filter or band-stop filter, to filter out 60 Hz as the body acts as a 60 Hz antenna, interfering with the heartbeat signal. The final design for the notch filter is a single-op-amp twin-t notch filter with 20+ dB of attenuation at 60 Hz, as shown in the schematic below.

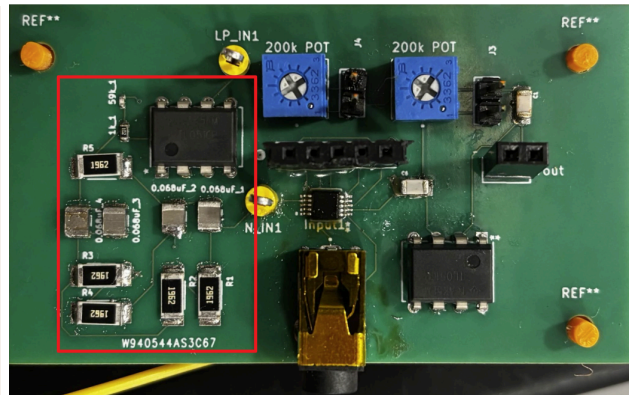
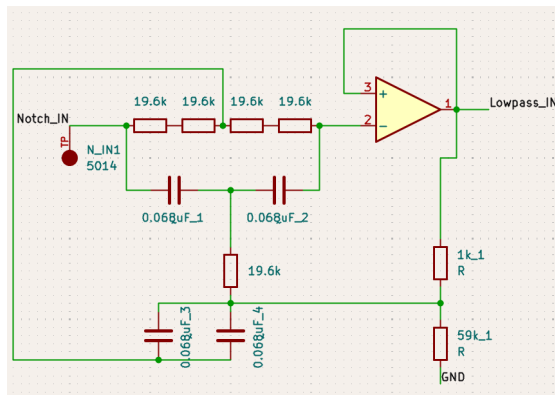


Figure 7: Notch Filter Schematic and Location on PCB

The third module is the second-order low-pass single-op-amp filter with a tunable cutoff. Its original 150 Hz cutoff was reduced to roughly 15 Hz based on guidance from the medical students, since even extreme heart rates (~300 bpm) occur near 5 Hz. To accommodate adjustment, we incorporated potentiometers for a variable cutoff.

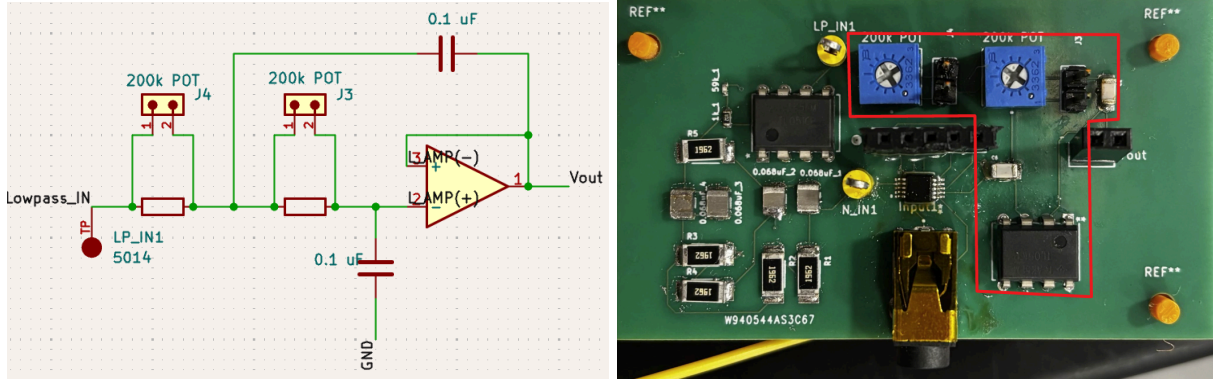


Figure 8: Low Pass Filter Schematic and Location

During testing, we found that the signal from the low-pass filter output was negative, which is not acceptable for the ESP32; thus, we added an inverting amplifier at the end, which did not make it onto the PCB.

2.2.2 Impedance

The impedance module underwent numerous design iterations. All in hopes of maintaining the current through the body resistance to under 100 μA . We began by just implementing the IC on a breadboard. This was implemented by hand-soldering the IC to a custom breakout board, as shown in Figure X, and then placing the breakout board on the breadboard for testing.

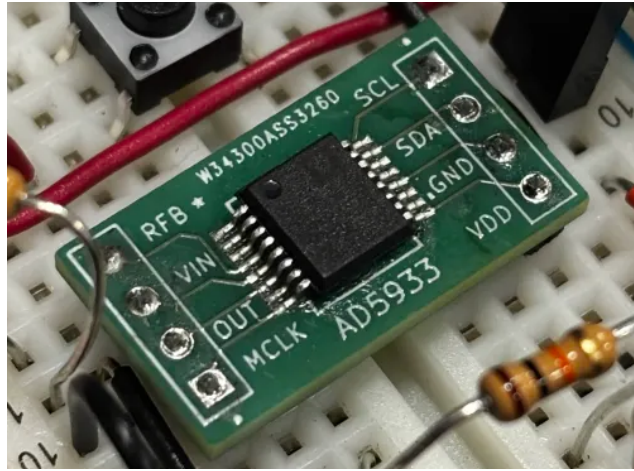


Figure 9: AD5933 Breakout Board

However, the IC cannot record impedances below 1 $\text{k}\Omega$ without external circuitry, as stated in the datasheet. Thus, we decided to redesign using transconductance amplifiers and instrumentation amplifiers to stay within current limitations and within the target resistance range, as shown in Figure 10 below, along with a functionality table in Table 1.

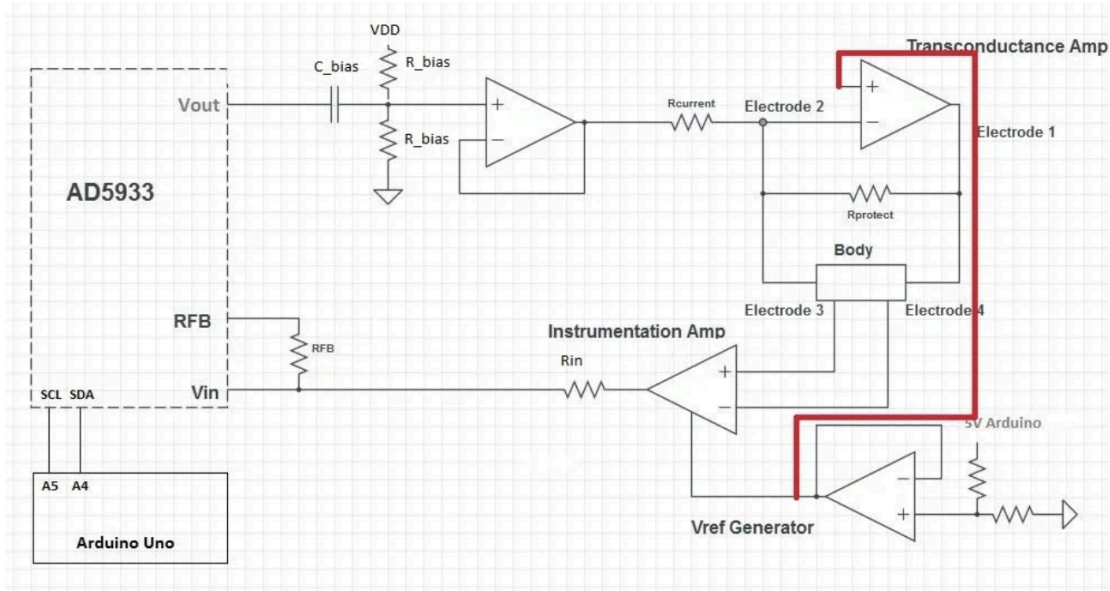


Figure 10: External Circuitry

Component	Expected Voltage	Expected Current
Output of Rebias Amp	$0.99 \sin(50,000t) + 1.65$	N/A
$R_{current} = 100,000 \Omega$	$0.99 \sin(50,000t)$	$\frac{0.99 \sin(50,000t)}{R_{current}} \approx 2 \mu App$
$R_{body} = (50, 5000) \Omega$	$R_{body}(50) * 2 \mu App = 0.1 mV$	$\frac{0.99 \sin(50,000t)}{R_{current}} \approx 2 \mu App$
Output of Instrumentation	$1mV \sin(50,000t) + 1.65$	$\frac{1mV \sin(50,000t)+1.65}{R_{fb} + R_{in}}$
R_{fb} / V_{in}	$-\frac{R_{fb}}{R_{in}} 1mV \sin(50,000t)$	$\frac{1mV \sin(50,000t)+1.65}{R_{fb} + R_{in}}$

Table 1: External Circuitry Functionality Table

Our initial testing of this circuit on the breadboard accurately measured impedances of 1k Ohms or higher, which remain outside our desired resistance range. After many tests, we determined that anything below 1k ohms results in a voltage signal too low for the impedance IC to detect.

To combat this, we opted for a different design that had never been tested before, as seen in Figure 11. Instead of sending current through the transconductance amplifier, it will pass through $R_{current}$ and then directly to ground via the pads. This signal will then pass through the instrumentation amplifier, with a gain of some value, to provide a readable voltage to the IC, with a DC offset of $VDD/2$.

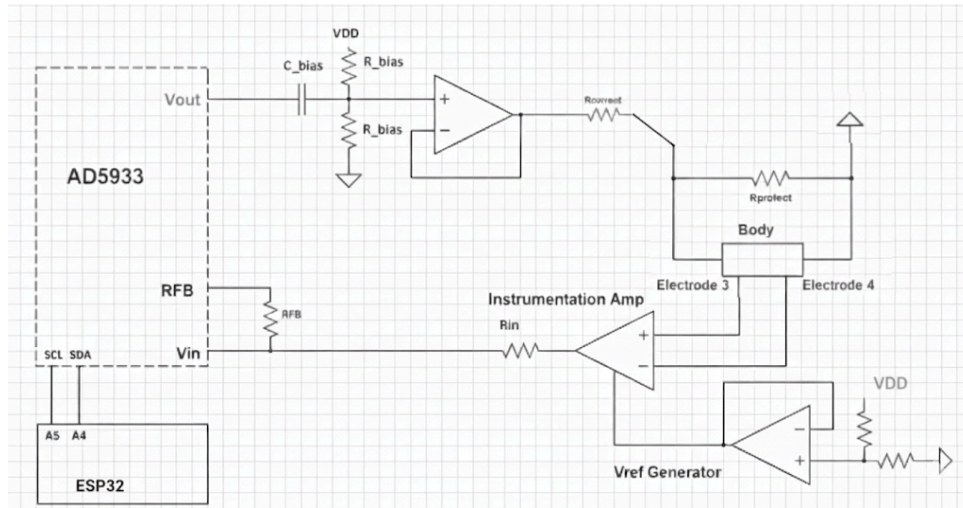


Figure 11: Redesigned External Circuitry

During the simulation of this new design, we observed a clear Ohm's law relationship between the peak-to-peak voltage and the change in body resistance. This was done by simulating a 50 kHz signal with a 2 Vpp at a DC offset of 1.48 through the circuit. This ultimately fell short because the IC could not interpret the circuit's reading, so we scrapped the idea entirely. For our demo, we reverted the design to the first iteration (Figure 12) and set the current to 10 kOhms to prevent the current from exceeding 20 uA at peak, as shown below.

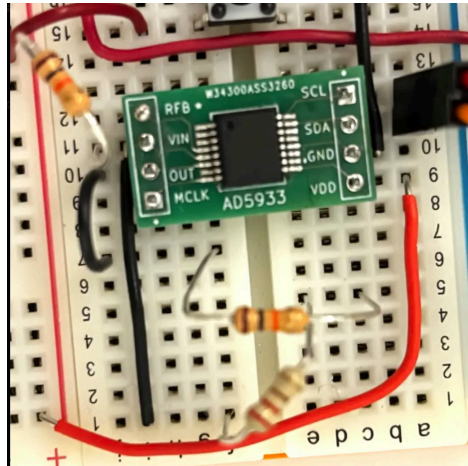


Figure 12: Demoed Topology

2.2.3 Power Unit

When properly implemented, we created our own design using isolated DC-DC converters, LDOs, and filtering capacitors, as explained earlier in the design procedures. We split it up into 3 sections: the boost section, the buck section, and the peripherals. The overall design is shown in the following figure.

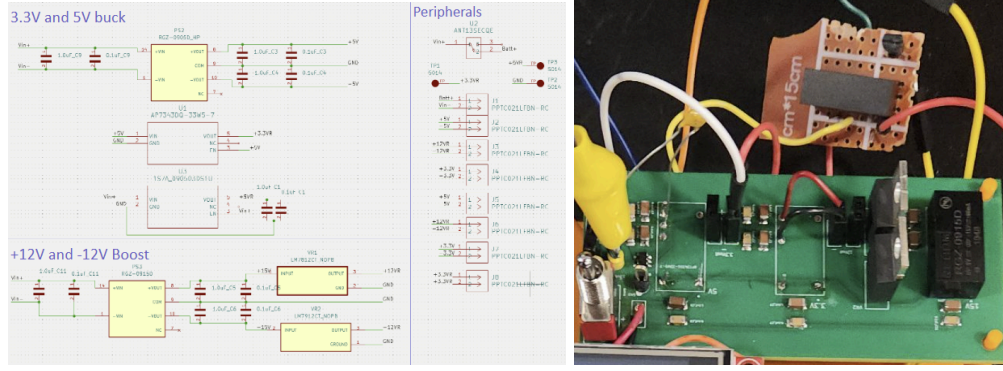


Figure 13: Power Board Schematic and PCB

Because we went with a modular approach, the powerboard needed multiple output channels to deliver the desired voltage to each subunit. We also incorporated a simple switch that would open-circuit the 9V battery when not in use, powering our design on and off.

The original PCB design we implemented, however, was built around different isolated DC-DC converters that were delayed and did not arrive within the project timeline. This required us to improvise and manually mount a similar, but not identical, part, as shown on the external patch board. We were able to integrate the functionality to achieve our desired outputs fully. When tested, the ripple voltage across the converter outputs was about $\pm 2V$, but with the decoupling capacitors added, it dropped to $\pm 100mV$, with spikes only at the switching frequency.

2.2.4 Control Unit

Only a few supplemental components were required to support the control unit's sensing and user interface features. These include hardware debounce for the mode-selection push button and an overvoltage protection stage on the ECG analog output to ensure compatibility with the 3.3 V input limit. Custom firmware works in tandem with these additions by handling mode switching, collecting ECG and impedance data, and driving the LCD interface.

Over-voltage Protection

The ECG subsystem outputs 1–2 V, but to prevent the ESP32 input from exceeding 3.3 V during voltage surges, a Zener diode clamp and 1 k Ω series resistor were added (Figure 14). The diode limits voltage to ~ 3.3 V, while the resistor restricts current to safe levels.

The resistor value was determined using Ohm's law:

$$R = \frac{V_{IN} - V_Z}{I} = \frac{5V - 3.3V}{1.5mA} \approx 1000\Omega \quad \text{Eq: 2}$$

Button Debounce

Mechanical buttons can produce multiple unintended transitions due to contact bounce. To prevent this, a debounce circuit was implemented (Figure 14) using an RC network with a 10 ms time constant, determined using the time-constant relation shown in (Eq. 3). A 10 k Ω resistor and 1 μF capacitor were selected to achieve this value. This provides clean transitions without noticeable input delay.

$$\tau = RC \quad \text{Eq: 3}$$

In this equation, τ represents the RC time constant, R is the resistance, and C is the capacitance.

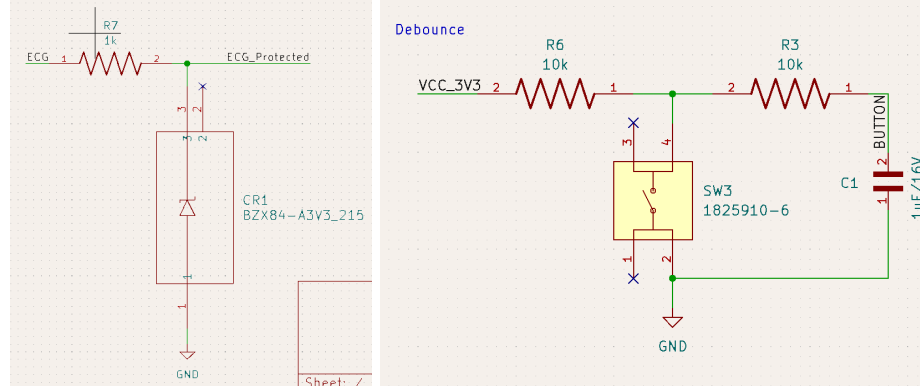


Figure 14: Overvoltage protection (left) and Debounce Circuits (right)

Software

The ESP32 microcontroller operates in two user-selectable modes, ECG and impedance, toggled via a push-button interrupt, with the default set to ECG mode. In ECG mode, the analog signal from the front-end is processed using a Pan-Tompkins-inspired algorithm to detect heartbeats. The signal is first bandpass filtered (5–15 Hz) to isolate QRS activity, then differentiated with a five-point derivative, squared to emphasize peaks, and integrated with a moving-window filter to generate a QRS envelope. Heartbeat detection utilizes an adaptive threshold calculated from the maximum of the most recent 300 samples, scaled by the magic number 0.04225. A QRS event is declared when the processed signal exceeds this threshold. Timestamps of detected QRS peaks are recorded using `millis()`, enabling RR intervals to be computed and stored in a buffer containing the ten most recent beats. The average RR interval is then used to calculate heart rate in BPM (see Equation 4). Δt is the average RR interval between the last ten detected heartbeats.

$$BPM = \frac{60}{\Delta t} \quad \text{Eq. 4}$$

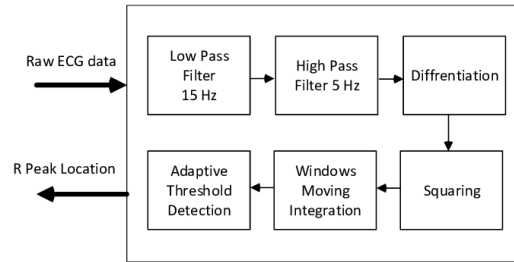


Figure 15: Pan-Tompkins QRS Detection Algorithm Flow Chart

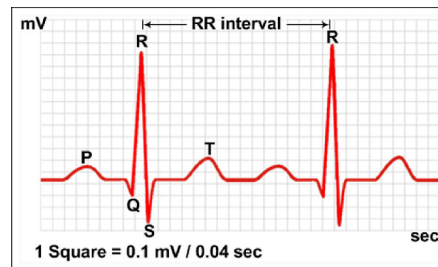


Figure 16: QRS Wave Graph

To display the calculated heart rate, the ESP32 updates the LCD using the Adafruit graphics library. This library manages all communication with the display, so the microcontroller only needs to send updated BPM values when they change. The screen is driven through an SPI interface, where the ESP32 transfers the required display data over a high-speed serial connection. By relying on the library to handle display communication, the ECG processing code stays focused on signal analysis while still providing real-time visual feedback of the heart rate.

In impedance mode, the system uses a modified version of the open-source AD5933 library developed by Meli (GitHub repository: [mjmel/arduino-ad5933](https://github.com/mjmel/arduino-ad5933)). The original example code sets up a frequency sweep by configuring parameters such as start frequency, frequency increment, number of increments, and the calibration resistor value. For this project, the code was simplified to perform a single impedance measurement at 50 kHz using a 10 k Ω calibration resistor instead of sweeping across multiple frequencies.

Although the library provided a usable measurement routine, the AD5933's impedance readings were not accurate on their own. The output was proportional to the actual impedance but needed calibration to match the returned value to a real-world measurement. To determine this relationship, several known resistors ranging from 100 Ω to 10 k Ω were measured, with ten readings taken for each value. These data points were used to fit a linear regression model and generate a calibration equation relating the library's output to the actual impedance, as shown in Figure 17. During operation, the measured impedance is processed through this calibration function, and the corrected value is then displayed on the LCD in the same way as in ECG mode.

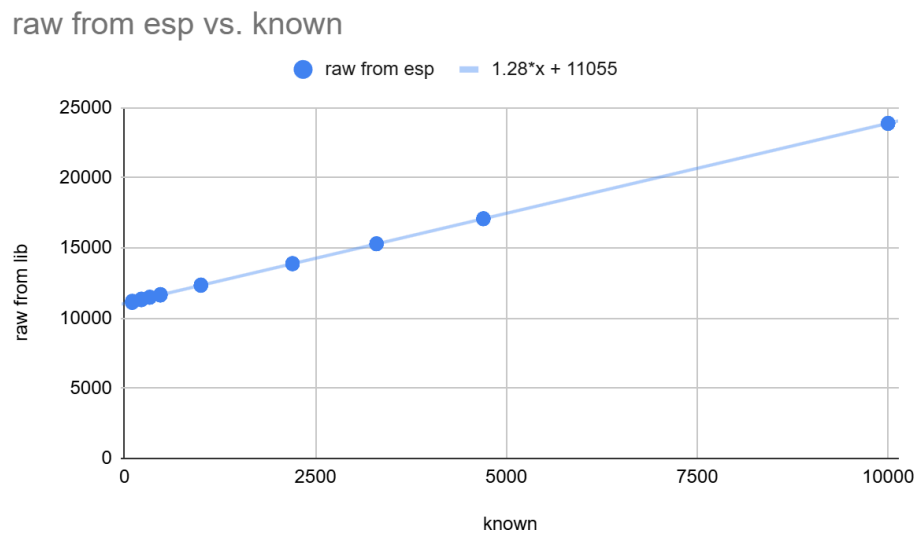


Figure 17: Linear calibration of AD5933 measurements versus known resistors.

3 Verification

3.1 ECG

Verification of the ECG was performed by comparing the ECG output with signals from a signal generator; later, we used our own hearts instead. We started with a signal generator, as illustrated by the large, fuzzy, green waveform. This signal was passed through the ECG, and the resulting clean sine wave is our output; the instrumentation amplifier's 1000-gain produced it. To verify the filters' effectiveness, we analyzed the signal's FFT to assess the strength of specific frequencies. As shown below, there are minor peaks at 60 Hz and 120 Hz, and their amplitudes are roughly equal, indicating that our filter effectively reduces the interference.

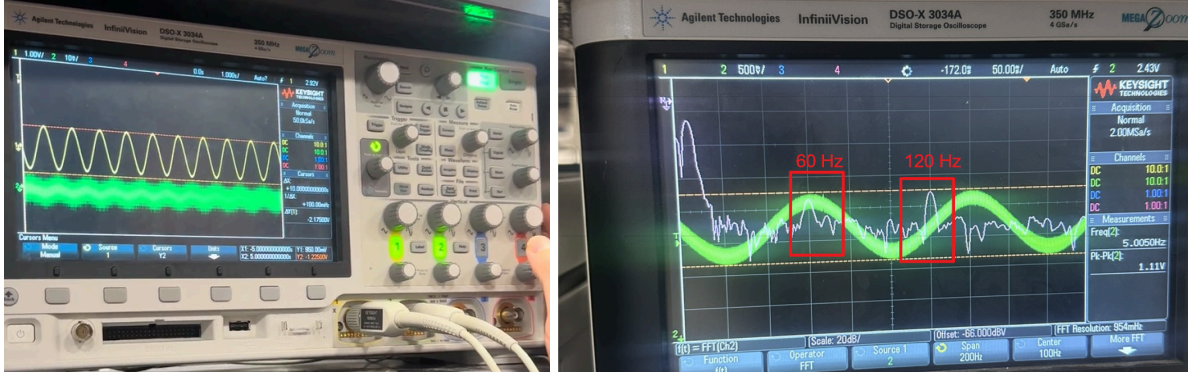


Figure 18: Verification of Instrumentation Amp and Filters

After verifying that the ECG performed well with the signal generator, we hooked it up to our hearts and successfully saw our heartbeat on the oscilloscope, as shown below.

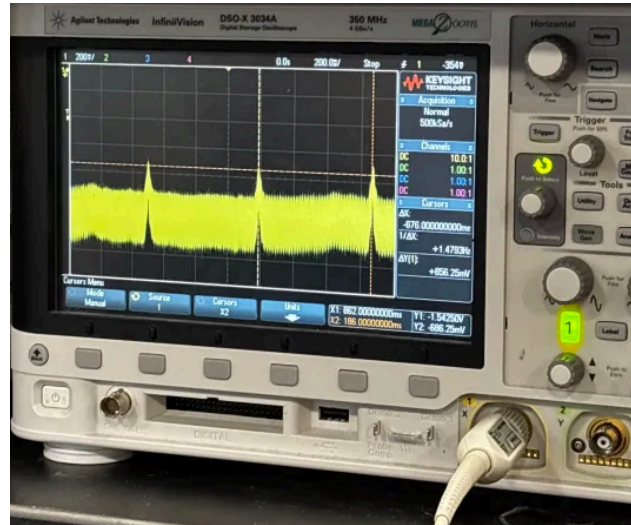


Figure 19: Testing on Heart

3.2 Impedance

The impedance module had two main requirements: measure impedances to within $\pm 5\%$ and limit current through the body resistor to no more than $100 \mu\text{A}$. To validate the resistances within $\pm 5\%$, we first measured the resistors' resistances with the multimeter, simulating body resistance, and then compared them to the AD5933 IC's measured post-processed values. At the same time,

we measured the voltage difference between the AD5933 output and the V_{in} input. Dividing by the $R_{current}$ plus simulated body resistance gives the current, and, as shown below (Table 2), it never exceeds 100 μA .

$R_{body} (\Omega)$	Measured Resistance (Ω)	Max Current across $R_{body} (\mu A)$
99.9	99.62	99.29789368
218.5	221.4	98.11694747
325.3	343.3	97.05882353
468.7	480.84	95.74468085
998.1	1012.7	91.07635695

Table 2: Resistance and Current Readings

3.3 Power Unit

To verify the power unit, we used an oscilloscope to measure the output voltages. When using the DC Ohm meter, it always showed the correct DC values, but to ensure stability, we needed to use more sensitive probes and examine waveform shapes. The shape of the +12V output can be seen in Figure 20:



Figure 20: +12 VDC output (left) and zoomed in on the high frequency ringing (right)

The average output voltage is +12V, with spikes at the isolated DCDC converter's switching frequency due to parasitic high-frequency ringing. Despite decoupling capacitors, finite ESR/ESL, and mounting inductance, complete suppression of these transients is achieved. The boost converter switches at 20kHz, but ringing occurs at 115kHz, higher than the switching frequency, as expected. To verify stability, we recorded voltage data at ringing points, summarized in Table 3.

Desired Output V	Average output (full screen)	Average Ripple	High Frequency Ring Pk-Pk	Spike width
+12V	12.027V	32.65mV	892.50 mV	135 ns

-12V	12.008V	33.75mV	782.25 mV	142 ns
+5V	4.9825V	27.87mV	632.64 mV	147 ns
+3.3v	3.2986V	15.57V	342.50 mV	156 ns

Table 3: Voltage Outputs

3.4 Control Unit

The control unit was tested to ensure that all primary functions in the Requirements and Verification Table operated as intended. Testing confirmed clean push button inputs, accurate heart rate and impedance measurements at 1 hertz, proper ECG processing, correct firmware operation, reliable calculation of average beats per minute, and smooth transitions between the Impedance Tracking and ECG states.

Debounce

To verify the debounce circuit's functionality, the output from Section 2.2.4 was connected to an ADALM2000 and observed using its oscilloscope. A trigger level of 1.5 V was set to capture the moment the button was pressed, allowing assessment of whether the debounce circuit produced a clean, continuous digital signal. For reference, Figure 21 shows the raw button signal without debouncing, while Figure 22 shows the resulting waveform from the ADALM2000, illustrating the smooth, continuous output after debouncing.

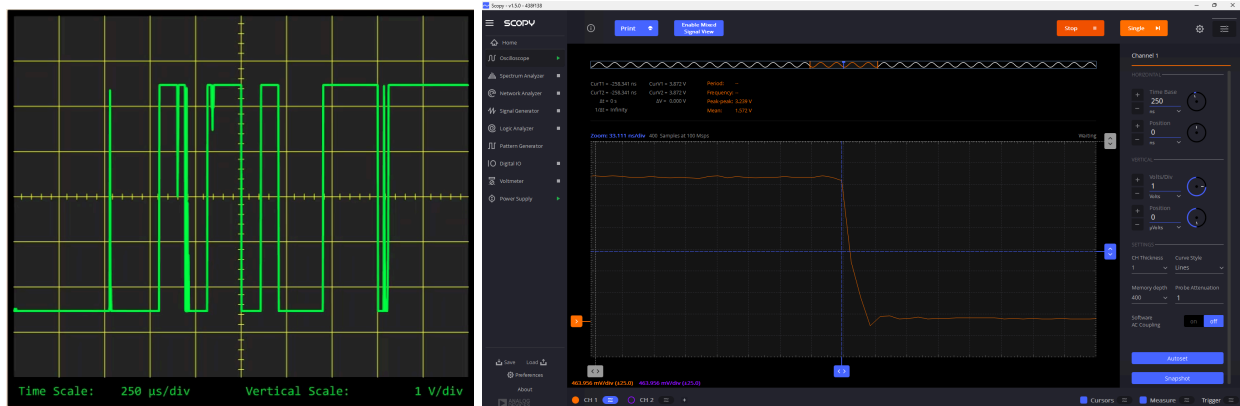


Figure 21: No Debounce (left) and with Debounce(right) Signal

LCD and Button Functionality

The qualitative verification of the control unit requirements demonstrates that the device behaves as intended during real-time operation. The heart rate and impedance values were displayed at a consistent 1 Hz update rate, and the measured heart rate was correctly computed using the average of the previous ten detected beats. During the final demonstration, a 1 Hz test waveform was applied to the ECG front end, and the display refreshed once per second, confirming accurate beat detection and correct screen update timing.

The event-driven firmware also operated as expected. The user interface reliably transitioned between ECG heart rate monitoring and impedance tracking whenever the push button was pressed. Each mode change was immediately reflected on the LCD screen, where the display

switched between BPM and impedance (see Fig. X), verifying proper state switching and robust handling of user inputs. These observations collectively confirm that the device fulfills its functional requirements for measurement accuracy, update timing, state management, and user-initiated mode selection.

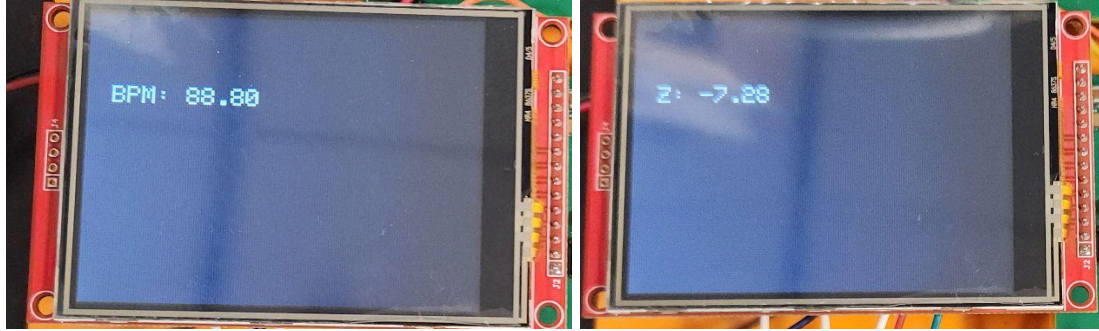


Figure 22: BPM (left) and Impedance (right) being displayed

Apply Digital Signal Processing to the ECG input

To demonstrate that the Pan–Tompkins heart-rate detection pipeline is functioning as intended, a simulated ECG-like signal was generated using:

$$x(t) = A\sin(2\pi t) + A\sin(100\pi t) \quad \text{Eq: 5}$$

with $A = 1V$. The 1 Hz component represents a clean heartbeat signal, while the 50 Hz component adds noise that the bandpass filter is intended to suppress. This waveform was injected into the software in place of the raw analog input. Figure 23 shows the unfiltered signal (blue) and the bandpass-filtered output (orange), where the 1 Hz waveform becomes clearly visible once the 50 Hz noise is removed. Because a 1 Hz signal corresponds to about 60 BPM, this also provides a direct check of the heart-rate calculation. To demonstrate the correct operation of the full Pan–Tompkins pipeline, Figure 23 also displays the derivative output, the squared signal, and the moving-window integration. The integrated waveform exhibits pronounced peaks aligned with the filtered 1 Hz signal, confirming that each stage of the algorithm behaves as expected.

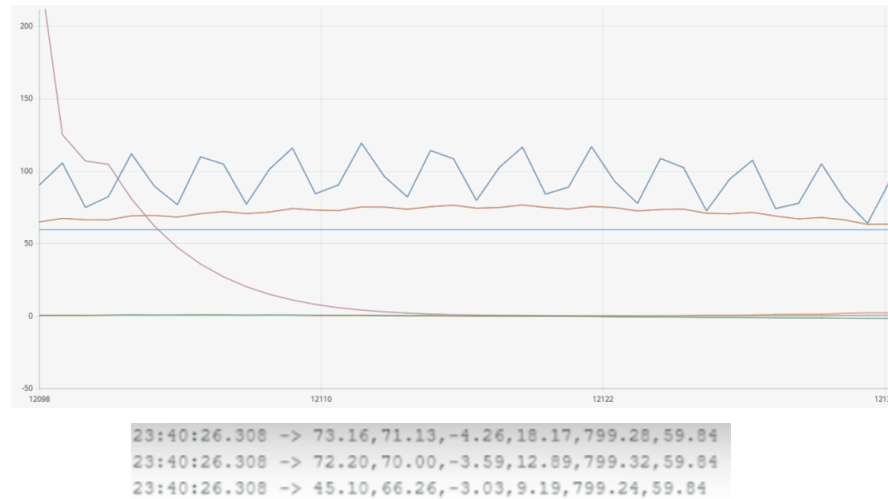


Figure 23: Pan–Tompkins processed ECG signal with BPM output on the bottom right

4 Costs and Schedule

The total cost of all parts we purchased is tabulated below, totaling \$187.89. This cost could have been significantly reduced if we had been more careful with our delicate parts and had not had to repurchase parts that were delayed beyond the project timeline. We estimated that each of us worked about 100 hours on this project during the semester at \$40 an hour. $(\$40/\text{hour}) \times 2.5 \times 100 \times 3$ This would yield a total of 30,000\$ in labor cost. This yields a total cost estimate of 30,187.89\$

Extended Price	Part Number	Description	Vendor	Qty	Unit Price
\$ 38.38	AD5933YRSZ-RE	IC DDS 16.776MHZ 12BIT 16SSOP	Digi-Key	2	\$ 19.19
\$ 12.03	919-RGZ-0915D	DC/DC Converters - Through Hole 2W DC/DC 3kV UNREG 9Vin +/-15Vout	Mouser Electron	1	\$ 12.03
\$ 6.13	5407-ESP32-S3-1	ESP32-S3-WROOM-1-N8R8	Digi-Key	1	\$ 6.13
\$ 4.95	1528-2659-ND	ADDRESS LED DISC SERIAL RGB 1=10	Digi-Key	1	\$ 4.95
\$ 3.80	P19.6KACCT-ND	RES SMD 19.6K OHM 1% 3/4W 2010	Digi-Key	10	\$ 0.38
\$ 3.64	3362P-204LF-ND	TRIMMER 200K OHM 0.5W PC PIN TOP	Digi-Key	4	\$ 0.91
\$ 3.27	445-2702-1-ND	CAP CER 0.1UF 50V COG 1210	Digi-Key	3	\$ 1.09
\$ 2.74	3386P-205LF-ND	TRIMMER 2M OHM 0.5W PC PIN TOP	Digi-Key	2	\$ 1.37
\$ 2.21	732-5960-1-ND	CONN RCPT USB2.0 MICRO B SMD R/A	Digi-Key	1	\$ 2.21
\$ 1.82	3362P-203LF-ND	TRIMMER 20K OHM 0.5W PC PIN TOP	Digi-Key	2	\$ 0.91
\$ 1.80	296-50628-ND	IC REG LINEAR 12V 1A TO220-3	Digi-Key	1	\$ 1.80
\$ 1.48	LM7912CT/NOPB	IC REG LINEAR -12V 1.5A TO220-3	Digi-Key	1	\$ 1.48
\$ 1.36	13-AC2010FK-07	RES SMD 324 OHM 1% 3/4W 2010	Digi-Key	8	\$ 0.17
\$ 1.28	478-KGM32ER7	CAP CER 1UF 16V X7R 1210	Digi-Key	2	\$ 0.64
\$ 1.20	S7000-ND	CONN HDR 2POS 0.1 TIN PCB	Digi-Key	5	\$ 0.24
\$ 1.18	660-RK73H2HRT	Thick Film Resistors - SMD 10K ohm 1% 0.75W AEC-Q200	Mouser Electron	2	\$ 0.59
\$ 1.12	S7008-ND	CONN HDR 10POS 0.1 TIN PCB	Digi-Key	2	\$ 0.56
\$ 0.90	13-RT0603BRCO	RES 500 OHM 0.1% 1/10W 0603	Digi-Key	2	\$ 0.45
\$ 0.80	1727-5309-6-ND	DIODE ZENER 3.3V 250MW TO236AB	Digi-Key	1	\$ 0.80
\$ 0.58	CL32A106KAULN	CAP CER 10UF 25V X5R 1210	Digi-Key	2	\$ 0.29
\$ 0.40	AP7343DQ-33W	IC REG LINEAR 3.3V 300MA SOT-25	Digi-Key	2	\$ 0.20
\$ 0.39	3372-LES05Z5.0	TVS DIODE 5VWM 16VC SOD523	Digi-Key	3	\$ 0.13
\$ 0.39	1825910-6	SWITCH TACTILE SPST-NO 0.05A 24V	Digi-Key	3	\$ 0.13
\$ 0.36	RMCF2010JT2M	RES 2M OHM 5% 3/4W 2010	Digi-Key	2	\$ 0.18
\$ 0.31	1N5819HW-FDK	DIODE SCHOTTKY 40V 1A SOD123	Digi-Key	1	\$ 0.31
\$ 0.30	311-10.0KFRCT-1	RES 10K OHM 1% 1/4W 1206	Digi-Key	3	\$ 0.10
\$ 0.26	541-0.0VCT-ND	RES SMD 0 OHM JUMPER 1/2W 1210	Digi-Key	2	\$ 0.13
\$ 0.20	541-100HCT-ND	RES SMD 100 OHM 1% 1/8W 0603	Digi-Key	2	\$ 0.10
\$ 0.10	YAG2296CT-ND	RES 1K OHM 1% 1/2W 1210	Digi-Key	1	\$ 0.10
\$ 15.10	LCD Display	LCD Display	Amazon	1	\$ 15.10
\$ 15.10	AD8253	Instrumentation Amplifier	Digi-key	3	\$ 45.30
\$ 11.70	AD622	Instrumentation Amplifier	Digi-key	3	\$ 35.10
\$ 11.64	RGZ-0915D	Isolated Module DC DC Converter 2 Output 15V -15V 8.1V - 9.9V Input	Digi-key	1	\$ 11.64
\$ 11.64	RGZ-0905D	Isolated Module DC DC Converter 2 Output 5V -5V 8.1V - 9.9V Input	Digi-key	1	\$ 11.64
\$ 11.64	RGZ-0903D	Isolated Module DC DC Converter 2 Output 3.3V -3.3V 8.1V - 9.9V Input	Digi-key	1	\$ 11.64
				Total	\$ 187.99

5 Conclusion

This project demonstrated an ECG and bioimpedance measurement device intended for future integration into a DSED. The system successfully reads heart rate and passive component impedance, displaying results on an LCD; however, the ECG is sensitive to movement and pad placement. The impedance module was validated on resistive loads but not tested on human subjects due to unverified current-safety protocols, demonstrating that while the core measurements are feasible, further testing is required for safe human use.

The project successfully measured heart rate and impedance within the allowable error range, and the results were displayed on the LCD. The main change over the semester was the LCD refresh rate, which did not affect measurement accuracy.

Some uncertainties remain. The ECG module is sensitive to patient movement and pad placement, and voltages outside 0–3.3 V can exceed the ESP32's input limits. The impedance module was only validated with passive resistors, as there was insufficient time and verified hardware to test it safely on human subjects. Future iterations could address these limitations by scaling input voltages, adding diode rectification, improving electrode placement and conductivity, and consolidating modules onto a single PCB.

Ethical Standards

The IEEE Code of Ethics requires prioritizing public safety, health, and welfare, and promptly disclosing any factors that may pose risks. Our team made sure to act lawfully, avoid conflicts of interest, reject bribery, provide and accept honest feedback, correct errors, make accurate claims, and give proper credit to others. We maintained technical competence and only undertook tasks for which we were qualified or disclosed any limitations of our device. For testing of the impedance measurement, which requires injecting a current of approximately 100 μA at 50,000 hertz, we did not perform any tests on humans because we were not certified to conduct such procedures.

6 References

- [1] Analog Devices, *Inverting Op Amp* (Glossary). [Online]. Available: <https://www.analog.com/en/resources/glossary/inverting-op-amp.html>
- [2] Analog Devices, “LT3471 Dual 1.3 A, 1.2 MHz Boost/Inverter in 3 mm × 3 mm DFN,” Datasheet, Rev. C. [Online]. Available: <https://www.analog.com/media/en/technical-documentation/data-sheets/lt3471.pdf>
- [3] Bourns, Inc., “TC33 Series 3 mm SMD Trimming Potentiometer,” Datasheet TC33. [Online]. Available: <https://www.bourns.com/docs/product-datasheets/tc33.pdf>
- [4] Espressif Systems, “ESP32 Hardware Design Guidelines.” [Online]. Available: <https://docs.espressif.com/projects/esp-hardware-design-guidelines/en/latest/esp32/index.html>
- [5] Espressif Systems, “ESP32-S3-DevKitC-1 v1.1 User Guide – Hardware Reference.” [Online]. Available: https://docs.espressif.com/projects/esp-dev-kits/en/latest/esp32s3/esp32-s3-devkitc-1/user_guide_v1.1.html#hardware-reference
- [6] GitHub, *arduino-ad5933 Repository*, by mjmeli. [Online]. Available: <https://github.com/mjmeli/arduino-ad5933>
- [7] Grainger College of Engineering, Univ. of Illinois, Urbana-Champaign, IL, “Safe Current Limits,” PDF. [Online]. Available: https://courses.grainger.illinois.edu/ece445/documents/Safe_Current_Limits.pdf
- [8] GreatScott!, “LCD Display Tutorial,” YouTube, 2018. [Online]. Available: <https://www.youtube.com/watch?v=EFAfcsYOrIM>
- [9] IEEE, “IEEE Policies, Section 7–8.” [Online]. Available: <https://www.ieee.org/about/corporate/governance/p7-8>
- [10] RECOM Power, “RJZ & RGZ 2 W Unregulated DC/DC Converters, DIP14 – Datasheet,” Rev. 3, 2024. [Online]. Available: https://recom-power.com/pdf/Econoline/RJZ_RGZ.pdf
- [11] ResearchGate, “Illustration of QRS Complexes and RR Interval of ECG Signals.” [Online]. Available: https://www.researchgate.net/figure/Illustration-of-QRS-complexes-and-RR-interval-of-ECG-signals_fig4_326588784
- [12] ResearchGate, “Pan and Tompkins Algorithm.” [Online]. Available: https://www.researchgate.net/figure/Pan-and-Tompkins-Algorithm_fig6_305698292

- [13] Texas Instruments, “LM2931-N Series Low Dropout Regulators,” Datasheet SNOSBE5G, Rev. G, Apr. 2013. [Online]. Available: <https://www.ti.com/product/LM2931-N>
- [14] Texas Instruments, “LM78Lxx 100-mA Fixed Output Linear Regulator,” Datasheet SNVS754K, Rev. K, Dec. 2016. [Online]. Available: <https://www.ti.com/product/LM78L05>
- [15] Texas Instruments, “TL05x, TL05xA Enhanced-JFET Low-Offset Operational Amplifiers,” Datasheet SLOS178A, Rev. A, Feb. 2003. [Online]. Available: <https://www.ti.com/lit/ds/symlink/tl051a.pdf>
- [16] Texas Instruments, “Video: Operational Amplifier Training Series.” [Online]. Available: <https://www.ti.com/video/5840441551001>
- [17] L. G. Tereshchenko and M. E. Josephson, “Frequency content and characteristics of ventricular conduction,” *J. Electrocardiol.*, vol. 48, no. 6, pp. 933–937, Nov.–Dec. 2015. Available: <https://pmc.ncbi.nlm.nih.gov/articles/PMC4241473/>
- [18] “AD8253: Dual, Low Noise, Low Power, Variable Gain Amplifier,” Analog Devices — Data Sheet, rev. ??, 20??. Available: <https://www.analog.com/media/en/technical-documentation/data-sheets/AD8253.pdf>
- [19] “Band-Stop (Notch) Filter — Tutorial,” *Electronics-Tutorials.ws*. Available: <https://www.electronics-tutorials.ws/filter/band-stop-filter.html>
- [20] “Second Order Low-Pass Filters — Tutorial,” *Electronics-Tutorials.ws*. Available: <https://www.electronics-tutorials.ws/filter/second-order-filters.html>
- [21] W.-Y. Yang et al., “ECG Voltage in Relation to Peripheral and Central Ambulatory Blood Pressure,” *Am. J. Hypertens.*, vol. 31, no. 2, pp. 178–187, Sep. 2017. Available: <https://pmc.ncbi.nlm.nih.gov/articles/PMC8031592/>
- [22] D. Hu, T. K. Cheng, K. Xie, and R. H. W. Lam, “Microengineered Conductive Elastomeric Electrodes for Long-Term Electrophysiological Measurements with Consistent Impedance under Stretch,” *Sensors*, vol. 15, no. 10, pp. 26906–26920, Oct. 2015. Available: <https://www.mdpi.com/1424-8220/15/10/26906>
- [23] “Electrocardiogram (ECG) Circuit — Instructables,” Instructables.com, published 3.0 years ago. Available: <https://www.instructables.com/Electrocardiogram-ECG-Circuit-3/>
- [24] “Bio Impedance Analysis (BIA) With the AD5933 — Instructables,” Instructables.com. Available: <https://www.instructables.com/Bio-Impedance-Analysis-BIA-With-the-AD5933/>

[25] “Electrical System for Bioelectric Impedance using AD5933 Impedance Converter,” A. Garcia & A. C. Sabuncu, Southern Methodist University, 2019. Available: <https://scholar.smu.edu/cgi/viewcontent.cgi?article=1049&context=jour>

7 Appendix

Requirement and Verification Tables

Electrocardiogram

Requirement	Specific Component	Verifications
The amplifier must amplify the signal roughly by 1000 times	Instrumentation Amplifier	<ul style="list-style-type: none">• Connect an oscilloscope to the input and the output of the amplifier to ensure amplification
The filter should cut out frequencies around 60 Hz, depending on the Q factor.	Notch Filter	<ul style="list-style-type: none">• Insert a parasitic signal of 60 Hz at the input of the notch filter; the output should not see the parasitic signal• Send a small range of frequencies to determine what frequencies are attenuated to match calculations
Frequencies outside of 150 Hz must be attenuated to nearly zero.	Low-pass Filter	<ul style="list-style-type: none">• Insert a parasitic signal greater than 150 Hz at the input of the low-pass filter; the output should not see the parasitic signal

Bio Impedance Tracking

Requirement	Specific Component	Verifications
Current across the body must be under 1 mA	R_{current}	<ul style="list-style-type: none"> • Connect a voltmeter to probe for voltage and current across a dummy resistor in place of R_{body}. • Test points over R_{current} to
Impedance reading must be within 5% of true value	R_{body}	<ul style="list-style-type: none"> • Compare with multimeter value across various resistors

Control System

Requirements	Verifications
The start/stop push button must produce clean digital signals without multiple unintended triggers (debouncing).	<ul style="list-style-type: none"> • Connect an oscilloscope to the button's output after the Schmitt trigger debounce circuit. • Press and release the button multiple times and verify single clean transitions without bounce artifacts.
The analog input from the ECG subsystem must not exceed 3.3 V to protect the ESP32 GPIO.	<ul style="list-style-type: none"> • Apply controlled overvoltage (e.g., 5 V) to the ECG input and measure voltage after the Zener clamp using an oscilloscope. • Confirm voltage is limited to ~3.3 V. • Verify current through the series resistor remains below 2.5 mA.
Must accurately display heart rate and impedance on the LCD at a refresh rate of 1 Hz.	<ul style="list-style-type: none"> • Connect known test signals to ECG and impedance inputs. • Observe LCD visually to verify data refresh at 1 Hz. • Cross-check displayed values against known inputs.
The control subsystem firmware must follow the event-driven flow shown in Figure X, ensuring proper initialization, waiting for user input, periodic sampling and processing, data display, and safe shutdown when the stop button is pressed.	<ul style="list-style-type: none"> • Review the source code to confirm the structure matches the flowchart • Observe system behavior in real time: the system should remain idle until the start button is pressed, then enter the sampling loop, update the display periodically, and return to the waiting state after the stop is pressed.
Apply Digital Signal Processing on the ECG	Utilizing Pan–Tompkins algorithm

input.	Algorithm, and a 2nd order butterworth bandpass digital filter we were able to entirely remove the residual noise that came from the slight output noise of the amplifiers within our ECG. To verify our algorithm is correctly assisting, we can connect an Arduino and a laptop to display the real-time effects of our DSP algorithm. We emphasize that these elements are NOT required for the functionality of our product; they are just there to verify the functionality.
Display an Average BPM, based on the previous 10 Beat pulses	After correctly identifying when heartbeats occur, we store the calculated time between the last 10 beats and calculate a beat per minute that is sent to our LCD display. We will have the AED pads attached to our body as we lie down to simulate a patient's conditions. We will use an Apple Watch to verify that the BPM is similar to the actual.
Utilization of ESP32 to switch freely between Impedance Tracking state and ECG State.	Press the button to see the modes switch

Power Regulation Unit

Requirement	Verifications
Supply power to all subsystems at rated currents and voltages.	The supply power should successfully step down the 9V battery voltage to 3.3V and 5V, respectively.
At maximum power draw, supply voltages should not drop.	The power supply for 3.3V should never diverge more than 0.2V when running under maximum load, meaning all other subunits are being powered. The 5V power supply should not diverge more than 0.5V.
Produce positive and negative 12V output for sensitive amplifying stages. Create a unified ground between all other sub-units.	Using an oscilloscope and ensuring that there is both positive and negative 12V when referred to the ground of the entire board.
Eliminate Output Voltage noise. Produce stable signals.	Using an oscilloscope, ensure the waveform shape has minimized peak-to-peak voltage, and that the voltage average does not deviate from the intended value.